Research Article
Journal of Advanced Development in Engineering and Science
Vol.16 ● No.46 • May – August 2026

The Study of Magnetic Levitation Force Using a Magnetic Railway Train Experimental Kit

Suppanyou Meakniti[1*], Pongkaew Udomsamuthirun[2], Tunyanop Nilkamjon[2], Sujittra Sangchaisee[3] And Thitipong Kruaehong[4*]

Received: 31 July 2025
Revised: 31 January 2026
Accepted: 27 April 2026

ABSTRACT

This study investigates the effects of magnetic pole orientation on the levitation performance of a model magnetic levitation (maglev) train. A physics instructional kit was developed to demonstrate electromagnetic principles through hands-on experimentation. The magnetic track was constructed using three distinct magnet arrangements: (1) all magnets oriented with the north pole facing upward, (2) all magnets oriented with the south pole facing upward, and (3) an alternating sequence of north–south poles. Examination of the resulting magnetic field lines revealed elevated field densities at the periphery of the track and at the interfaces between adjacent magnetic poles. The train base was configured in six arrangements (A1-1, A1-2, A1-3, A2-1, A2-2, and A2-3), employing two different sizes of neodymium magnets. The experimental results demonstrated a nonlinear decrease in magnetic lift force as the distance between the magnets increased. Within the 0–1 cm range, configurations featuring uniform pole orientation (A1-1, A1-2, A2-1, and A2-2) produced greater lift forces than those with alternating pole arrangements (A1-3 and A2-3), with the maximum and minimum recorded forces being 0.7 N and 0.08 N, respectively. These findings highlight the strong influence of pole alignment on lift efficiency and suggest that uniform magnetic orientation enhances levitation performance.

Keywords: Magnetic Levitation Force; Magnetic Field; Magnetic Railway Train

[1]General Science Program, Faculty of Education, Suratthani Rajabhat University, Suratthani, Thailand 84100
[2]Department of Physics, Faculty of Science, Srinakharinwirot University, Bangkok, Thailand 10110
[3]Science Center, Faculty of Science and Technology, Suratthani Rajabhat University,Thailand 84100
[4]Department of Industrial Electrics, Faculty of Science and Technology, Suratthani Rajabhat University,Thailand 84100
*Corresponding author e-mail: thitipong.kru@sru.ac.th

Introduction

Understanding scientific knowledge is essential for developing students' cognitive abilities. It promotes critical skills such as analytical thinking, logical reasoning, and the practical application of scientific concepts [1]. A strong foundation in science encourages active student participation in scientific inquiry, connecting classroom learning with research and the creation of new knowledge. Moreover, scientific thinking helps learners apply their understanding to real-world problems, aligning with 21st-century educational goals that emphasize essential competencies for life and work [2]. This study focuses on improving students' comprehension of complex scientific topics, particularly magnetic fields. These abstract concepts often require imaginative teaching methods that bridge theoretical ideas and observable phenomena. However, teaching magnetic field concepts poses challenges, especially due to the high cost of experimental equipment. Many schools lack the resources to provide hands-on learning opportunities, which negatively affects students' engagement and academic achievement [3]. In recent years, technological innovations have become increasingly important in physics education [4]. Physics, which explores the principles of nature, can be particularly difficult for students when it comes to topics like electromagnetism [5]. Concepts such as magnetic fields, forces, and motion within magnetic environments are hard to visualize, making it difficult for learners to build accurate mental models. Effective instruction requires teaching tools that make abstract ideas more concrete and understandable. Traditional lecture-based approaches may not adequately support deep learning in this area.

Electromagnetism is a fundamental topic in physics and underpins the development of numerous technologies, including electrical devices, communication systems, and transportation methods. Designing experimental activities that simulate real-world applications helps students connect theory with practice. Hands-on experiences with electromagnetic phenomena [6-8], such as Faraday's Law and magnetic force, provide students with meaningful learning opportunities that strengthen their understanding and prepare them for future academic or technical pursuits. A key application of electromagnetic theory is the magnetic levitation (Maglev) train. This system uses magnetic fields for both levitation and propulsion, allowing the train to float above its track without physical contact. The underlying principles are explained by Maxwell's Equations, which describe how electric currents generate magnetic fields and how these fields interact [9-10]. In Maglev trains, Lenz's Law [11] describes the repulsive forces that allow the train to levitate. The propulsion system of a Maglev train relies on electromagnetic induction. Coils along the track carry alternating current (AC), which reverses direction continuously and creates a changing magnetic field. This dynamic field interacts with magnets on the train: the front section of the track produces an attractive force by opposing the polarity of the train's magnets, while the rear section generates a repulsive force with the same polarity, pushing the train forward [12-14].

This study applies the principle of magnetic repulsion to design and construct a prototype magnetic levitation (Maglev) system, demonstrating stable levitation through the lift force generated by interactions between permanent magnets [15–16]. The structure of the magnetic track and the levitating base was designed in various configurations to investigate the effects of magnet orientation, pole spacing, and polarity arrangement on the lift force and system stability. The analysis focuses on understanding magnetostatic interactions and the mechanism of quasi-stable levitation that occurs without active electronic control. The developed structure serves as a practical model for applied physics research on magnetic force phenomena. In addition, Zhou et al. [17] investigated the underlying mechanisms and dynamic characteristics of repulsive permanent magnetic levitation systems, demonstrating that stable, zero-power levitation can be achieved through magnetostatic interactions without active electronic control. Their analytical and experimental results provide theoretical support for understanding the influence of magnet arrangement on levitation force behavior.

Materials and Methods

This study involves the design and development of an instructional tool in the form of a magnetic railway system, aimed at enhancing students' foundational understanding of electromagnetic theory, with a particular emphasis on magnetic force. By integrating real-world applications of electromagnetism, the tool bridges theoretical concepts with practical phenomena, thereby promoting a more tangible and intuitive learning experience compared to conventional instructional methods that progress linearly from theory to application. The research focuses on examining magnetic levitation behavior under varied experimental conditions, specifically through different configurations of magnetic track and base alignments. These configurations include north–north (N–N), south–south (S–S), and north–south (N–S) arrangements, where "N" and "S" denote the respective magnetic poles. Magnetic lift force measurements were conducted at multiple distances to assess the effects of these configurations. Two sizes of flat rectangular neodymium magnets were employed in the construction of the train base: type A1 (20 mm × 60 mm × 5 mm) and type A2 (20 mm × 100 mm × 5 mm). Six magnet configurations were created, three using four A1 magnets and three using two A2 magnets. The A1 configurations included: A1-1 (all north poles upward), A1-2 (all south poles upward), and A1-3 (alternating north and south poles). Similarly, the A2 configurations comprised: A2-1 (both north poles upward), A2-2 (both south poles upward), and A2-3 (alternating north and south poles). These configurations are illustrated in Figure 1.

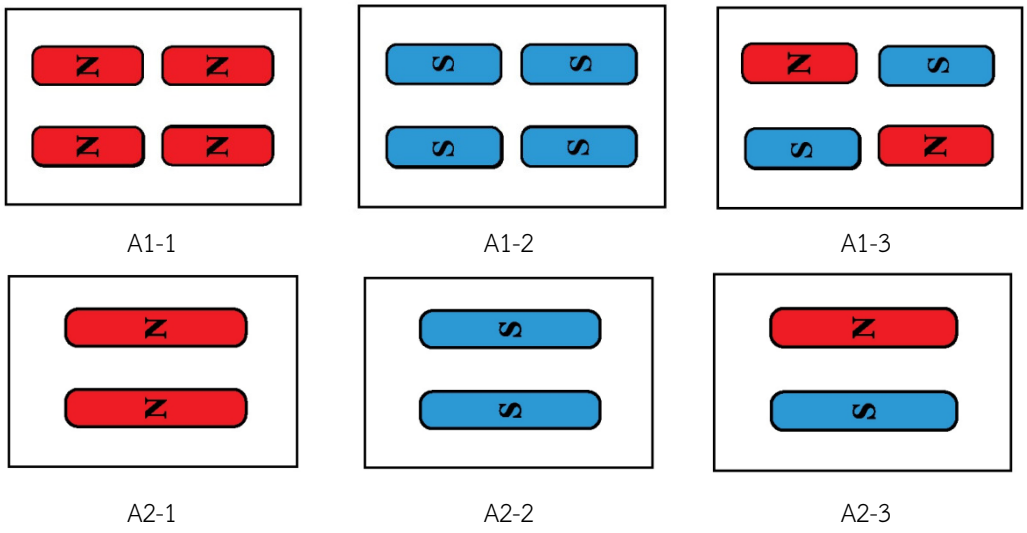
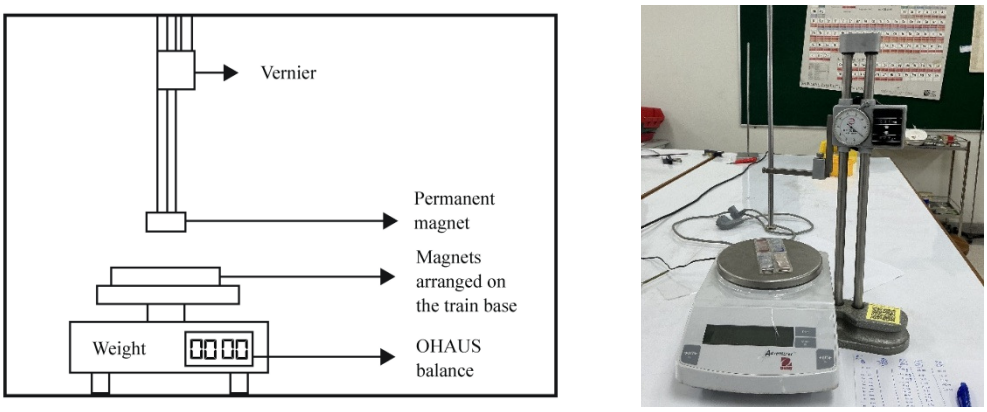


Figure 1 The arrangement of neodymium magnets at the base of the train head in configurations A1-1, A2-1, A3-1, A1-2, A2-2, and A.3-2

The six magnet configurations were selected to represent two principal magnetic pole orientations relevant to magnetic levitation systems: uniform pole alignment and alternating pole alignment. Uniform configurations were intended to enhance repulsive magnetic interaction and levitation stability, while alternating configurations were designed to investigate magnetic field cancellation and flux confinement effects that may reduce lift force. This systematic design allows evaluation of both optimal levitation performance and practical limitations in magnet arrangement.

The magnetic levitation force in the experimental setup was quantified using an OHAUS precision scale, as illustrated in Figure 2. Measurements were conducted for the train head equipped with a magnetic base arranged in six distinct configurations: A1-1, A1-2, A1-3, A2-1, A2-2, and A2-3. The procedure involved positioning a permanent magnet sheet, exhibiting a magnetic flux density of 38.8 mT, at a fixed initial distance of 1 cm from the surface of the magnetic base, representing the nearest point at which magnetic repulsion occurred. The sheet was then displaced away from the magnetic base in 1 cm increments up to a maximum distance of 13 cm. The process was subsequently reversed, with the sheet moved toward the magnetic base from 13 cm back to 1 cm in the same incremental steps. This bidirectional measurement allowed for the assessment of magnetic levitation force across varying distances for each configuration. Additionally, the magnetic field lines

associated with each base configuration were examined using a magnetic field visualization kit to support further analysis of the magnetic field distribution.



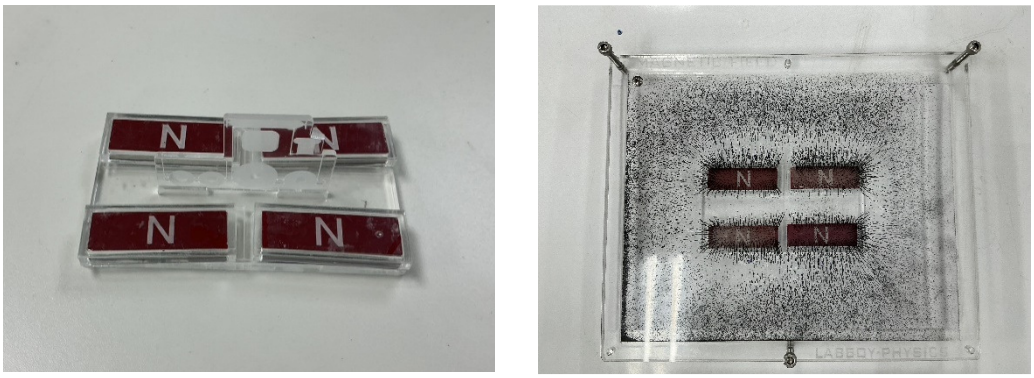
(a) (b)

Figure 2 (a) Equipment setup for measuring levitation force and (b) Levitation force measurement using an OHAUS scale.

Results and Discussion

In the A1-1 configuration, four neodymium magnetic bars, each measuring 20×60×5 mm, were arranged with all north poles facing upward, as illustrated in Figure 3(a). To examine the magnetic field behavior, a magnetic field visualization kit was used, revealing the distribution of magnetic field lines associated with this configuration (Figure 3(b)). Magnetic levitation force measurements were conducted at distances ranging from 1 cm to 13 cm, at three distinct positions spaced 3.5 cm apart along the magnetic base. At each point, three measurements were recorded, and the average value was used for analysis.

The results, depicted in Figure 4, show the variation in levitation force with distance for the A1-1 configuration. The data series F-1, F-2, and F-3 correspond to measurements taken at the three specified positions. The graph indicates that the levitation force peaks at very short distances (approximately $r \approx 0-1$ cm), after which it declines sharply as the distance increases beyond 1 cm. A slight secondary rise in levitation force is observed in the range of $r = 2-4$ cm, followed by a gradual decrease approaching zero at distances greater than 4 cm. The force-distance profiles for F-1, F-2, and F-3 exhibit consistent trends, suggesting that the levitation force values were comparable across the three measurement positions.



(a) (b)

Figure 3 (a) The train head base arranged in the A 1-1configuration and (b) The magnetic field lines of the train head base arranged in the A 1-1configuration.

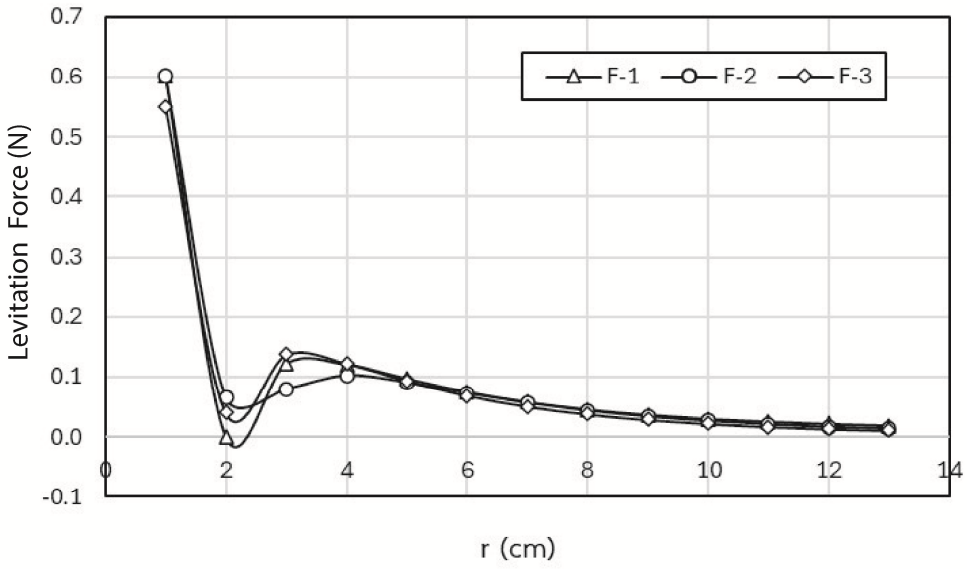
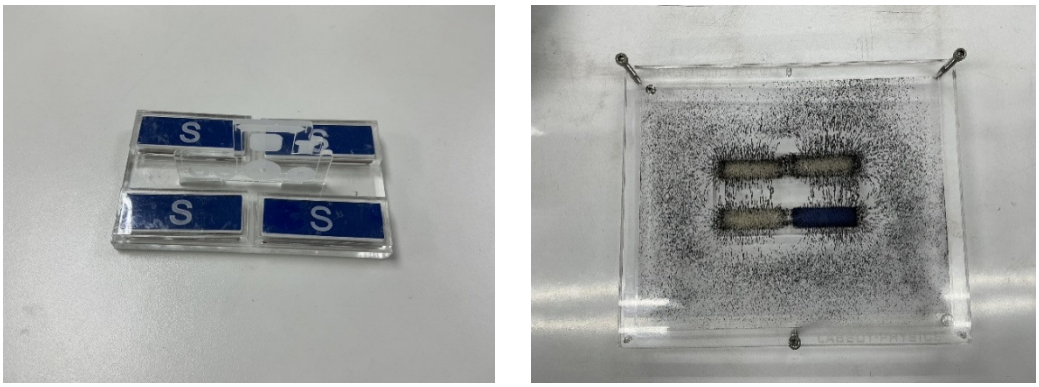


Figure 4 Magnetic levitation force in the A 1-1magnet arrangement.

In the A1-2 configuration, four neodymium magnetic bars, each measuring 20×60×5 mm, were arranged with their south poles oriented uniformly upward, as shown in Figure 5(a). The corresponding magnetic field distribution was examined using a magnetic field visualization kit, with the resulting field line patterns depicted in Figure 5(b). Magnetic levitation force measurements were conducted at three distinct locations along the track, spaced 3.5 cm apart. At each location, measurements were taken at intervals ranging from

1 cm to 13 cm, with three trials per point. The average levitation force at each distance was computed and used for analysis.

The relationship between levitation force and vertical separation for the A1-2 configuration is illustrated in Figure 6, where F-1, F-2, and F-3 correspond to the three measurement positions. The results indicate that the levitation force reached its maximum, approximately 0.7 N, at the shortest distance ($r \approx 0-1$). The force then declined sharply as the distance increased. A slight secondary increase in levitation force was observed in the intermediate range ($r = 2-4$), followed by a gradual reduction approaching zero at distances beyond 6 cm. All three measurement points exhibited consistent trends, with negligible variation in levitation force among the positions.



(a) (b)

Figure 5 (a) The train head base arranged in the A 2-1configuration and (b) The magnetic field lines of the train head base arranged in the A 2-1configuration.

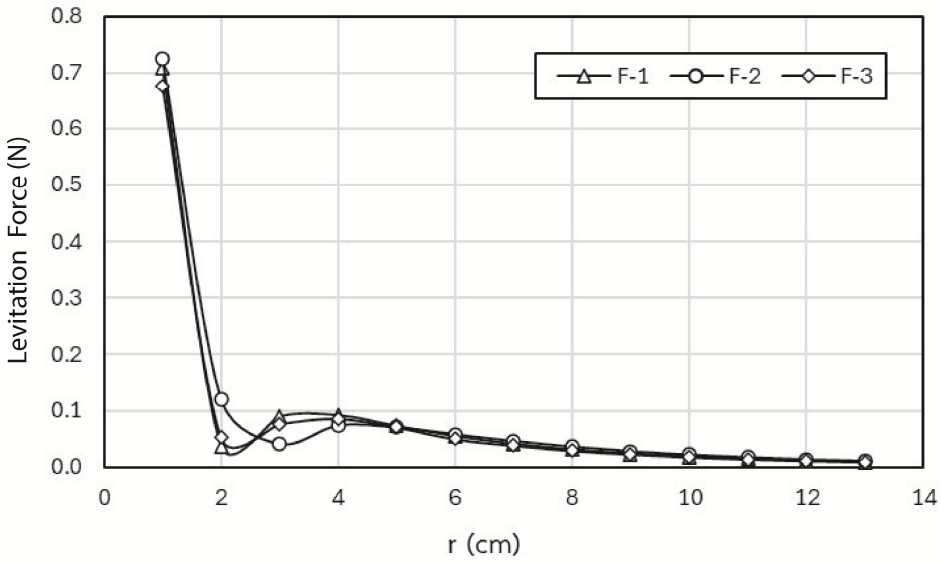
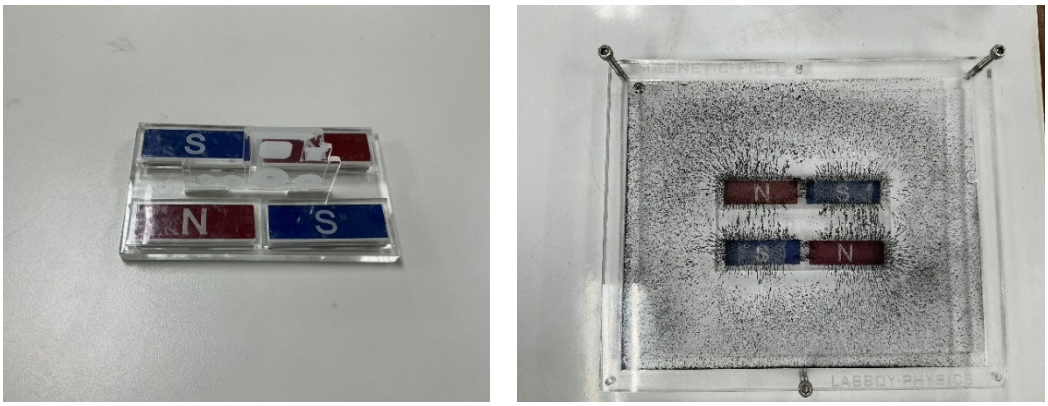


Figure 6 Magnetic levitation force in the A-12magnet arrangement.

In the A1-3 configuration, four neodymium magnetic bars, each with dimensions of 20×60×5 mm, were arranged in an alternating north–south pole orientation, as depicted in Figure 7(a). The magnetic field distribution associated with this configuration was examined using a magnetic field visualization kit, with the resulting field line patterns illustrated in Figure 7(b). Magnetic levitation force measurements were performed at three discrete positions along the track, each spaced 3.5 cm apart. Measurements were recorded at distances ranging from 1 cm to 13 cm, with three repetitions at each point, and the mean values were used for analysis.

The relationship between levitation force and distance for the A1-3 arrangement is presented in Figure 8, with data series F-1, F-2, and F-3 corresponding to the respective measurement positions. The results show that the levitation force reached a peak of approximately 0.08 N within the range of $r \approx 0-1$ cm. Beyond this point, the force rapidly diminished, approaching zero at distances exceeding 6 cm. All three datasets demonstrated similar overall trends, with only minor variations in peak force values and the rate of force decay. No substantial differences in levitation force were observed among the three measurement positions.



(a) (b)

Figure 7 (a) The train head base arranged in the A-13configuration and (b) The magnetic field lines of the train head base arranged in the A-13configuration.

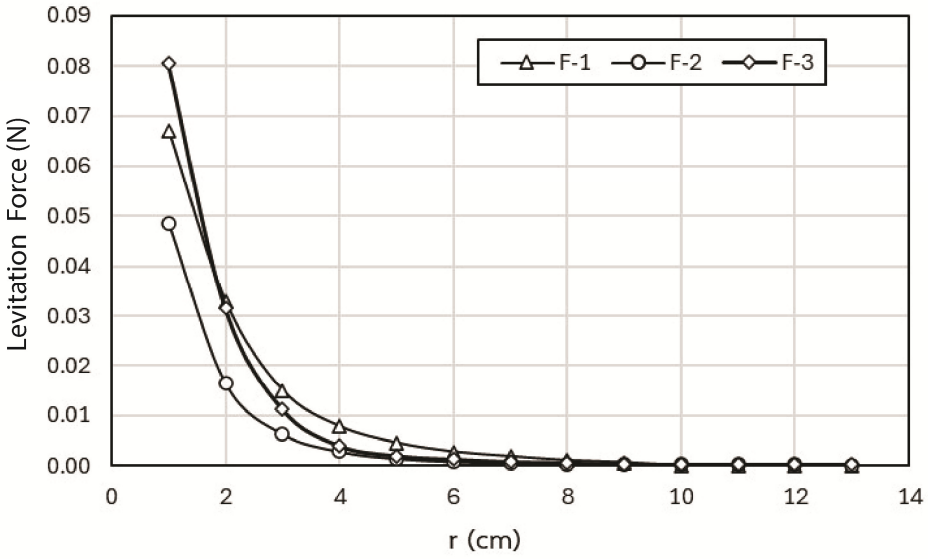
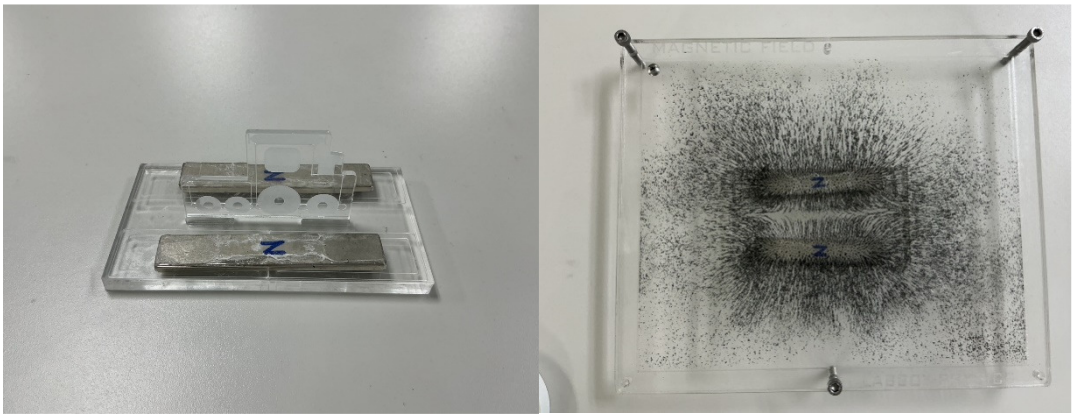


Figure 8 Magnetic levitation force in the A-13magnet arrangement.

In the A2-1 configuration, two neodymium magnetic bars, each measuring 20×100×5 mm, were arranged with their north poles uniformly oriented upward, as illustrated in Figure 9(a). The magnetic field distribution generated by this configuration was examined using a magnetic field visualization kit, and the resulting field line patterns are presented in Figure 9(b). Magnetic levitation forces were measured at three distinct positions along the magnetic

base, spaced 3.5 cm apart. At each position, measurements were conducted at intervals ranging from 1 cm to 13 cm, with three repeated trials at each point. The average levitation force at each distance was calculated and used for subsequent analysis.

The relationship between levitation force and vertical distance for the A2-1 configuration is shown in Figure 10, where F-1, F-2, and F-3 correspond to the three measurement locations. The results reveal that the levitation force reached a maximum of approximately 0.6 N at the shortest measured distance ($r \approx 0-1$), followed by a sharp decline as the distance increased. A modest secondary rise in levitation force was observed between $r = 2-6$, after which the force gradually decreased, approaching zero at distances beyond 12 cm. The data from all three positions exhibited consistent patterns, indicating that the levitation force values were comparable across the measurement points.



(a) (b)

Figure 9 (a) The train head base arranged in the A2-1configuration and (b) The magnetic field lines of the train head base arranged in the A2-1configuration.

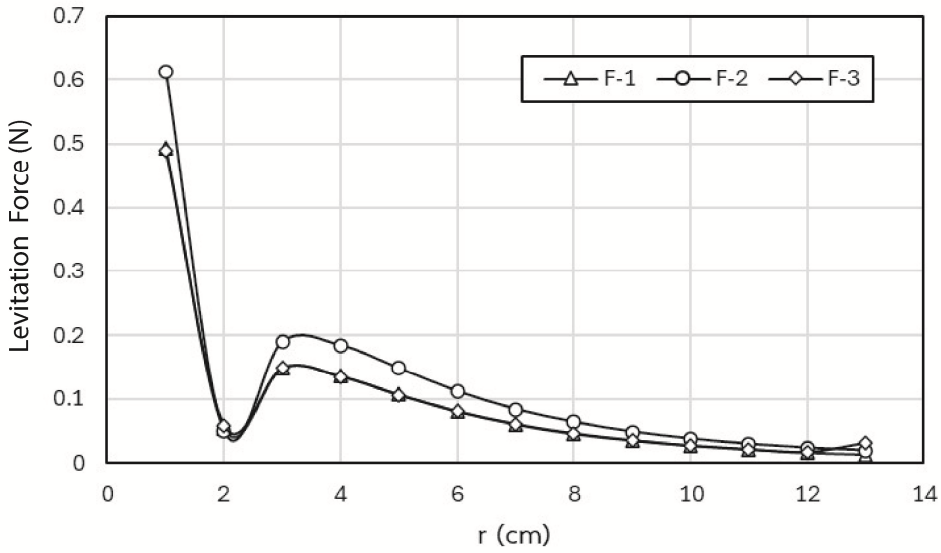
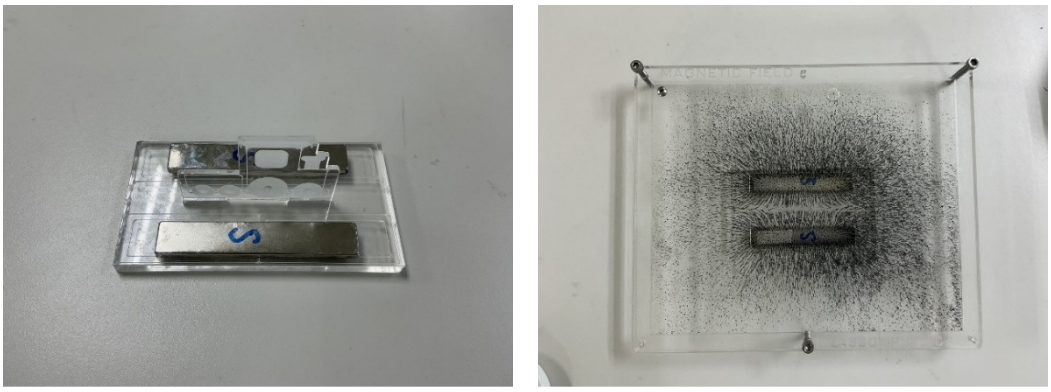


Figure 10 Magnetic levitation force in the A2-1magnet arrangement.

In the A2-2 configuration, two neodymium magnetic bars, each with dimensions of 20×100×5 mm, were arranged with their south poles uniformly oriented upward, as depicted in Figure 11(a). The magnetic field distribution for this configuration was investigated using a magnetic field visualization kit, with the observed field lines presented in Figure 11(b). Magnetic levitation force measurements were carried out at three distinct positions along the magnetic base, each separated by 3.5 cm. At each position, force data were collected across distances ranging from 1 cm to 13 cm in 1 cm increments, with three repeated measurements per point. The average force value at each distance was computed for analysis.

The relationship between levitation force and distance for the A2-2 arrangement is shown in Figure 12, where the curves labeled F-1, F-2, and F-3 correspond to the three measurement points. The data indicate that the levitation force peaked at approximately 0.7 N in the initial range of $r \approx 0 - 1$ cm, followed by a sharp decline with increasing distance. In the range of $r = 2 - 4$ cm, the levitation force stabilized around 0.1 N before gradually decreasing further, approaching zero at distances beyond 6 cm. All three datasets demonstrated consistent trends, indicating that the levitation force values were comparable across the measurement locations.



(a) (b)

Figure 11 (a) The train head base arranged in the A2-2configuration and (b) The magnetic field lines of the train head base arranged in the A2-2configuration.

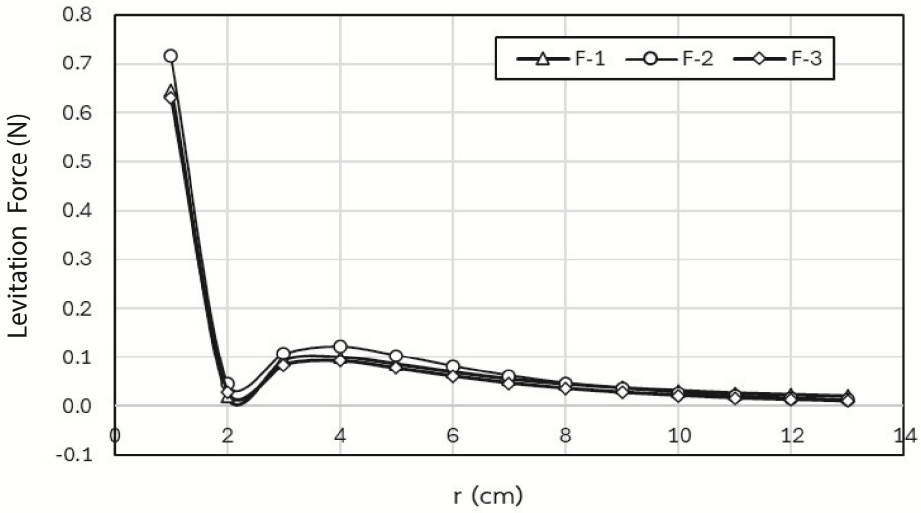
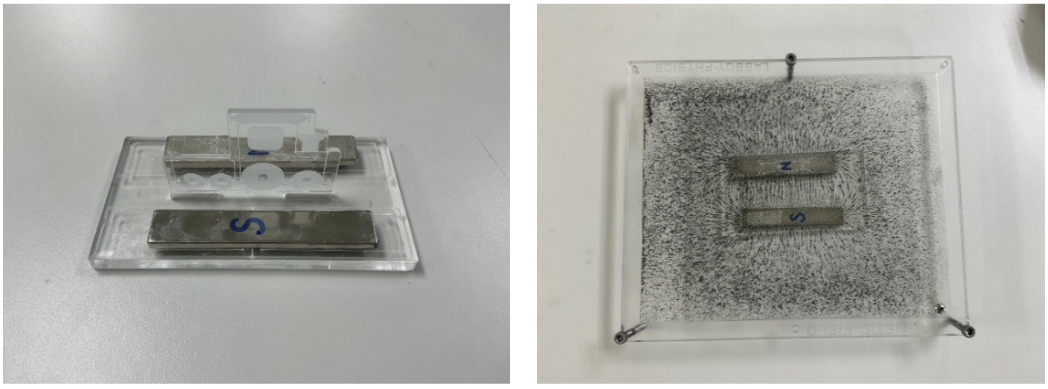


Figure 12 Magnetic levitation force in the A2-2magnet arrangement.

In the A2-3 configuration, two neodymium magnetic bars, each measuring 20×100×5 mm, were arranged in an alternating north–south pole orientation, as illustrated in Figure 13(a). The corresponding magnetic field distribution was examined using a magnetic field visualization kit, with the resulting field lines depicted in Figure 13(b). Magnetic levitation force measurements were conducted across distances ranging from 1 cm to 13 cm at three discrete positions along the magnetic base, each spaced 3.5 cm apart. For each position, three measurements were taken, and the average values were used for analysis.

The relationship between levitation force and distance for the A2-3 configuration is presented in Figure 14, where F-1, F-2, and F-3 denote the levitation forces recorded at the three respective positions. The results indicate that the maximum levitation force, approximately 0.14 N, occurs at a short distance near $r \approx 0-1$ cm. Beyond this point, the force declines sharply. Within the range of $r = 2-4$ cm, the levitation force approaches zero and remains nearly constant at a negligible level beyond 6 cm. All three data sets exhibit consistent patterns, indicating that the levitation force values were comparable across the measurement points.



(a) (b)

Figure 13 (a) The train head base arranged in the A2-3configuration and (b) The magnetic field lines of the train head base arranged in the A2-3configuration.

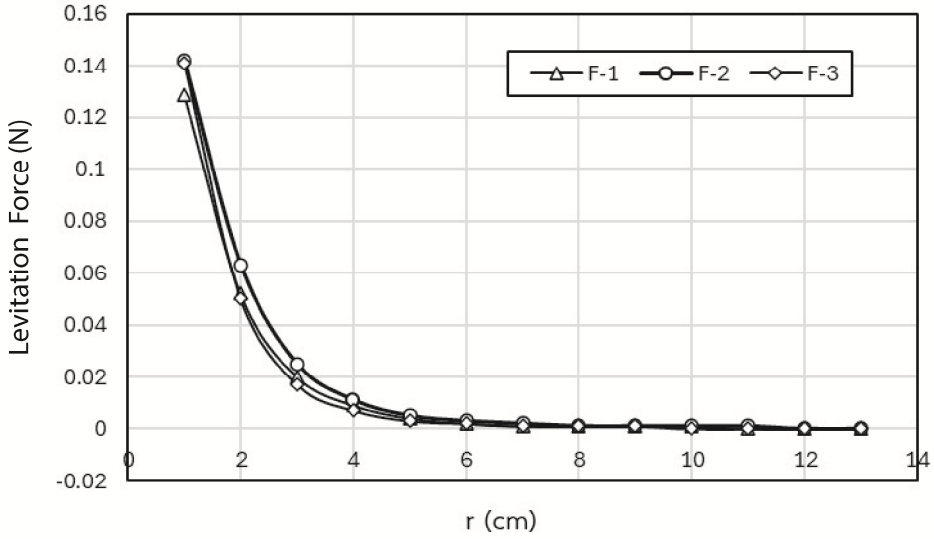


Figure 14 Magnetic levitation force in the A-23magnet arrangement.

In the A1-1 (all north poles facing upward) and A1-2 (all south poles facing upward) configurations, the measured levitation force peaked within a short range ($r \approx$ 0-1 cm), reaching approximately 0.6-0.7 N. The force rapidly decreased as the distance increased. This behavior aligns with the inverse square nature of magnetic forces, where the strength of the interaction diminishes with increasing separation between magnetic sources. The consistency of levitation force across all measurement points also reflects a relatively uniform magnetic field distribution generated by the aligned polarity. The visualization of the magnetic field lines for these configurations revealed strong vertical repulsive interactions above the magnets. The resulting magnetic lift is primarily caused by the direct repulsion between like poles in the opposing magnet sheets, forming the core mechanism of levitation in this passive system. The A1-3 configuration, consisting of alternating north and south poles, exhibited closed-loop magnetic field lines within the magnet array. This internal field containment led to a reduced external field, and hence a lower lift force. The maximum levitation force recorded was approximately 0.08 N at the closest distance, decreasing to near zero beyond 6 cm. These results indicate that alternating pole arrangements are less effective in producing external lift forces in passive magnetic systems.

Configurations A2-1 and A2-2 used longer neodymium magnets (100 mm) with uniform pole alignment. Their levitation behavior was similar to A1-1 and A1-2, but with slightly increased lift force near the shortest gap. The increased magnet size contributed to a broader magnetic surface area, enhancing the resulting lift force, which again peaked around 0.6–0.7 N. The magnetic field remained consistently distributed, as in the smaller-magnet configurations. In configuration A2-3, alternating north–south poles were arranged using the larger magnets. The maximum levitation force was approximately 0.14 N, still lower than the uniform polarity configurations. This outcome suggests that pole arrangement has a greater influence on lift force than magnet size in this system, where lift is driven primarily by the extent and direction of the external magnetic field.

Comparing all six configurations, it was found that uniform polarity arrangements yielded higher levitation forces than alternating ones. This can be attributed to the constructive alignment of magnetic fields in uniform configurations, which enhances the net upward force. In contrast, alternating arrangements result in partial cancellation of adjacent fields, reducing the effective lift. The nonlinear decrease in levitation force with distance agrees with fundamental magnetic theory. In some cases, the behavior may resemble dipole–dipole interactions, where the force decreases with the fourth power of distance $F \propto \frac{1}{r^4}$. Minor fluctuations in lift within the 2-4 cm range may be attributed to overlapping fringe fields or field redistribution near the magnet edges.

The observed trend of higher levitation force at short distances follows fundamental magnetic interaction behavior, where the force rapidly decreases with increasing separation

distance. Similar behavior is observed in magnetic suspension systems, where uniform pole arrangements enhance repulsive interaction and system stability. Compared with electromagnetic levitation systems, permanent magnet-based configurations offer simpler design and lower energy consumption, making them suitable for educational and small-scale applications.

Conclusions

This study examined the effects of magnetic pole orientation on levitation performance using six configurations of neodymium magnet arrangements on a model train: A1-1, A1-2, A1-3, A2-1, A2-2, and A2-3. Each configuration differed in magnetic pole alignment to determine its influence on the magnitude and stability of the lift force. The results showed that uniform pole arrangements, where all magnets face the same direction (either all north or all south), consistently produced stronger and more stable levitation. Maximum lift forces of 0.6 newtons (A1-1 and A2-1) and 0.7 newtons (A1-2 and A2-2) were observed at short distances (0–1 cm). In contrast, alternating pole configurations (A1-3 and A2-3) yielded much lower force values of 0.08 and 0.14 newtons, respectively. This reduction is attributed to the confinement of magnetic field lines within the array, reducing the strength of the external repulsive field. Therefore, the developed maglev train kit serves not only as a useful tool for investigating magnetic force interactions but also as an effective instructional resource for teaching electromagnetic concepts in physics.

The experimental results showed that the alternating magnetic pole configurations resulted in lower levitation force values compared to the uniform configurations. A clear decreasing trend was observed; however, statistical hypothesis testing was not conducted, and the findings are presented as indicative experimental observations.

References

[1] Habermas, J. (2015). *Knowledge and Human Interests*. John Wiley & Sons.

[2] Guo, J., & Woulfin, S. (2016). Twenty-First Century Creativity: An Investigation of How the Partnership for 21st Century Instructional Framework Reflects the Principles of Creativity. *Roeper Review*, *38*(3), 153–161.

[3] Cucos, C., & Iucu, R. (2020). Management of Continuous Training Programs for Teachers: Practical Guide. *Educatia 21*, *19*, 193–196.

[4] Galili, I. (2018). Physics and Mathematics as Interwoven Disciplines in Science Education. *Science & Education*, *27*(1–2), 7–37.

[5] Thipwan, M., et al. (2021). Construction of a Simple Alternative Current (AC) Magnetic Field Meter for Classroom Teaching. *Journal of Science and Technology Mahasarakham University*, *40*(2), 220-225. (in Thai)

[6] Dori, Y. J., & Belcher, J. (2005). Learning electromagnetism with visualizations and active learning. In J. K. Gilbert (Ed.), *Visualization in science education* (pp. 187–216). Springer.

[7] Schwichow, M., et al. (2016). What Students Learn From Hands-on Activities. *Journal of Research in Science Teaching*, *53*(7), 980–1002.

[8] Gillet, D., et al. (2001). Hands-on Laboratory Experiments in Flexible and Distance Learning. *Journal of Engineering Education*, *90*(2), 187–191.

[9] Liu, Z., et al. (2015). *Maglev Trains*. Springer.

[10] Tandan, G. K., et al. (2015). A Review on Development and Analysis of Maglev Train. *International Journal of Research in Advent Technology*, *3*(12), 14–17.

[11] Hooge, C. (2016). *BCIT Physics 0312 textbook*. British Columbia Institute of Technology.

[12] Chen, I. G., et al. (1998). Magnetic Levitation Force of Single Grained YBCO Materials. *Chinese Journal of Physics*, *36*(1), 2–11.

[13] Yang, J. H., et al. (2010). Development of Magnetic Force Modeling Equipment for Magnetic Levitation System. In *The 10th International Conference on Control, Automation and Systems (ICCAS 2010)* (p. 29–33). 27–30 October 2010, Gyeonggi-do, South Korea.

[14] Livingston, J. D. (2011). *Rising Force: The Magic of Magnetic Levitation*. Harvard University Press.

[15] Kruaehong, T., et al. (2009). The Construction of Maglev Train Model. *SWU Science Journal*, *25*(2), 91–100. (in Thai)

[16] Chang, P. Z., et al. (1990). Levitation Force and Magnetic Stiffness in Bulk High-Temperature Superconductors. *Journal of Applied Physics*, *67*(9), 4358–4360.

[17] Zhou, F., et al. (2024). Study of Repulsive Permanent Magnetic Levitation Mechanism and Its Dynamic Characteristics. *Scientific Reports*, *14*, 81439.